7

Study of Degradation Products and Degradation Pathways of ECD and Its Drug Product, ECD Kit

Kung-Tien Liu, Yu-Yung Lin, Yi-Chih Hsia, Jian-Hua Zhao,
Chang-Yung Su, Shang-Yu Shen, Lee-Chung Men and Lie-Hang Shen
Institute of Nuclear Energy Research
Taiwan

1. Introduction

Recently, researchers have shown an increased interest in the investigations of drug stability and degradation pathway. Baertschi (2006) and Alsante et al., (2007) described an overall strategy for the prediction, identification and control of stability-related issues in active pharmaceutical ingredients (APIs) and drug products using stress testing. Forced degradation studies are part of the drug development strategy being undertaken to elucidate the intrinsic stability of the drug. Such studies are conducted under more severe and exaggerated conditions than those usually used for long-term stability tests. These studies are particularly useful to establish the drug degradation pathway and validate the suitable analytical procedures (Jocić et al., 2009).

Technetium-99m ethyl cysteinate dimer (Tc-99m-ECD or bicisate) is one of the most essential single-photon emission computed tomography (SPECT) imaging agents. In according to the practice guidelines of the American College of Radiology (ACR) (Abdel-Dayem, 2003) and the European Association of Nuclear Medicine Neuroimaging Committee (ENC) (Kapucu et al., 2009), clinical indications of Tc-99m-ECD include in evaluating the regional cerebral blood flow (rCBF) in patients with cerebrovascular diseases, transient ischemic attack, various forms of dementia, symptomatic traumatic brain injury, encephalitis, vascular spasm following subarachnoid hemorrhage, inflammation, epileptic foci and lacunar infarctions.

More indications of Tc-99m-ECD in SPECT brain perfusion imaging of neuropsychiatric disorders and chronic fatigue syndrome have not been fully characterized (Abdel-Dayem, 2003; Kapucu et al., 2009). However, investigations of the conversion in patients of mild cognitive impairment to Alzheimer's disease (AD) (Borroni et al., 2006), the functional compensation mechanism in incipient AD (Caroli et al., 2010), the mechanism for suppression of parkinsonian tremor by thalamic stimulation (Wielepp et al., 2001), the mechanism by which thyroid hormone availability affects cerebral activity (Schraml et al., 2006), brain glucose metabolism in hypothyroidism (Bauer et al., 2009), reduction in the bifrontal regions and diffusion-weighted imaging of Creutzfeldt-Jacob disease (Sunada et al., 2004; Ukisu et al., 2006), quantitation and differentiation in patients with Tourette's syndrome (Diler et al., 2002; Chen et al., 2003; Sun et al., 2001) and abnormal rCBF in patients with Sjögren's syndrome (Chang et al., 2002) were reported.

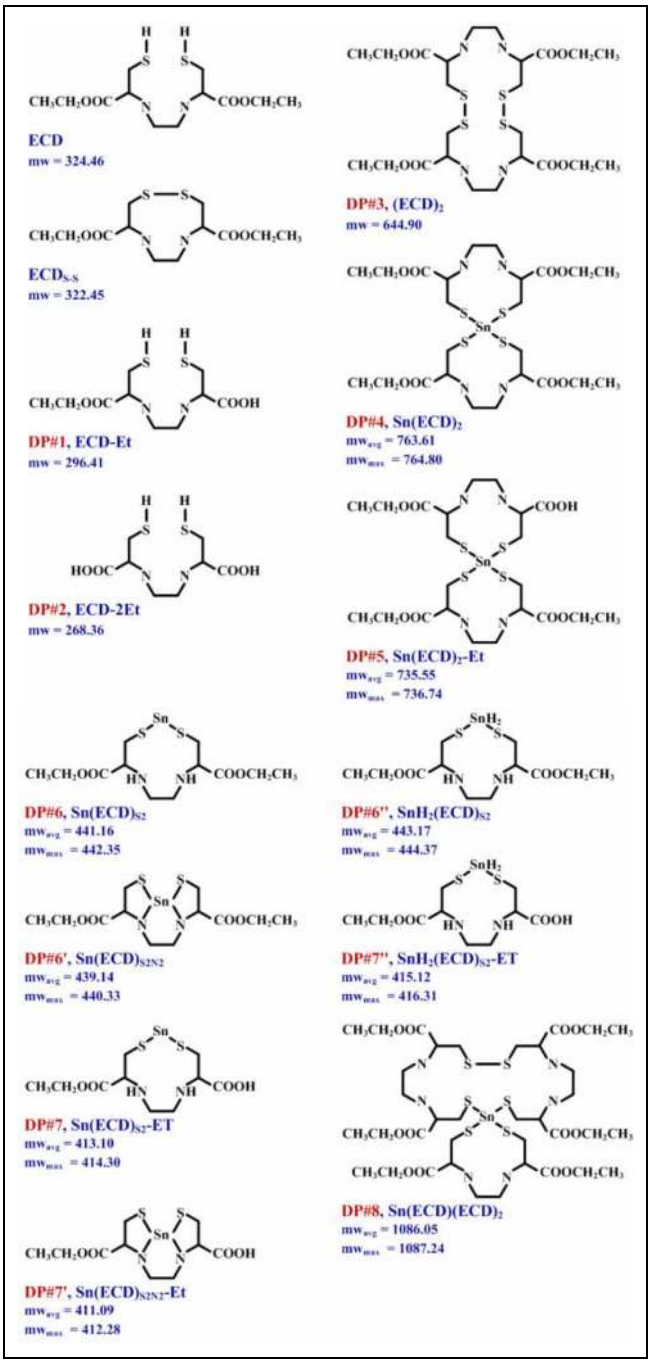

Fig. 1. Chemical structures of ECD and its DPs

For clinical implements, Tc-99m-ECD is obtained by radiolabeling of Tc-99m to its API, i.e. *L*-Cysteine, *N,N'*-1,2-ethanediylbis-, diethyl ester, dihydrochloride (ECD) (Fig. 1). Despite its safety and efficacy, a major drawback for the application of Tc-99m-ECD is the stability of ECD Kit in aqueous solution. For example, no more delay for patient injection that longer than 30 minutes is recommended by ACR and EANM (Abdel-Dayem, 2003; Kapucu et al., 2009).

So far, several studies investigating stability and degradation of ECD and Tc-99m-ECD have been reported, but there is still insufficient data for the elucidation of degradation products (DPs) structure and pathway. Mikiciuk-Olasik et al. (2000) demonstrated that ECD decomposed as soon as it was dissolved in phosphate buffer solutions. However, they offered no explanation for the structures of three decomposition products. Verduyckt et al. (2003) investigated the identity of Tc-99m-ECD using radio-LC-MS and reported five DPs for ECD including disulfide, monoacid monoester (ECM), diacid (EC) and Sn(IV) complexes with ECD (Sn-ECD) and EC (Sn-EC) derivatives. However, no systematic degradation study was reported to investigate the degradation mechanism or pathway on ECD Kit. The study of Tsopelas et al. (2005) was mainly focused on the behavior of Tc-99m and its reactions with components of ECD Kit.

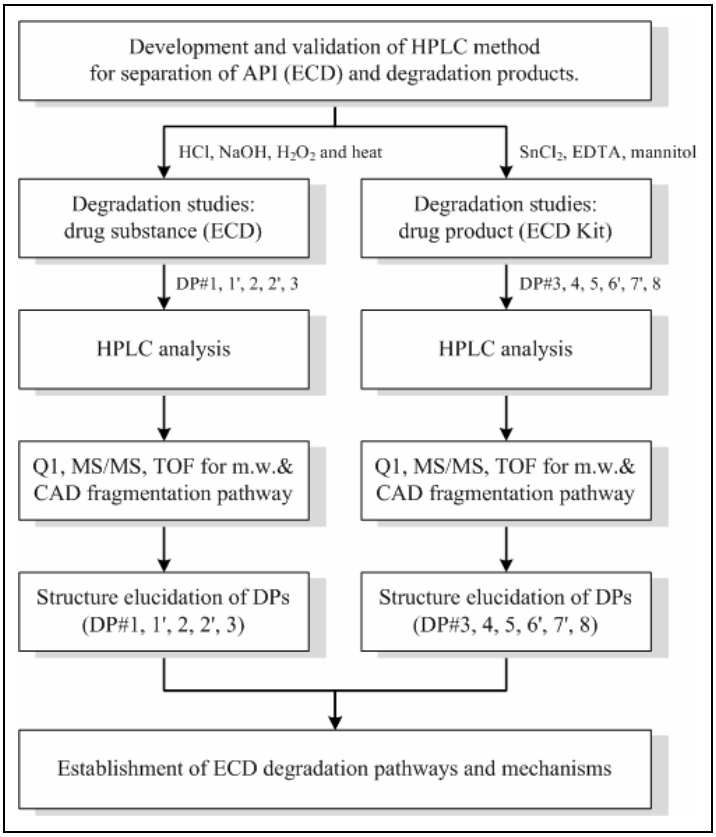

Fig. 2. Overall scheme for the ECD and ECD Kit degradation studies

Our preliminary observations showing that ECD Kit is highly unstable in (non)aqueous solution and the composition of ECD Kit is the major obstacle to determine stability of ECD (Chao et al., 2011). Therefore, the aim of this paper is to evaluate degradation kinetics and mechanism of ECD Kit in aqueous solution. No previous reports were found in the literature regarding the degradation behavior of ECD. The main issues addressed in this study were modified according to the procedures outlined by Shah et al. (Shah & Singh, 2010; Shah, et al., 2010; Raijada et al., 2010). The overall scheme in this degradation investigation (Fig. 2) includes: (i) development and validation of an HPLC method for determination of ECD and DPs, (ii) implement of the degradation and stress studies on ECD and ECD Kit, (iii) analysis of the DPs by HPLC, (iv) characterization of the molecular weights and collision activated dissociation (CAD) fragmentation pathways of ECD and DPs by Q1, MS/MS and TOF, (v) elucidation of the DPs' structures and (vi) establishment of the ECD degradation pathways and decomposition mechanisms.

2. Experimental

2.1 Materials and reagents

ECD (purity: 97.53%) was obtained from ABX (Radeberg, Germany). All chemicals and reagents were of analytical grade and used as received without further purification. Methanol (MeOH) (HPLC grade) was obtained from Merck (Darmstadt, Germany). Deionized water was purified using a Smart DQ3 reverse osmosis reagent water system (Millipore, MA, U.S.A.) with a 0.22-μm filter, TOC < 5 ppb, resistivity ≥ 18.2 MΩ-cm and endotoxin < 0.001 EU/mL.

2.2 HPLC instrumentation

An Agilent 1100 series high performance liquid chromatography (HPLC) (Agilent, Palo Alto, CA, U.S.A.) was employed, consisting of an on-line degasser, binary pump, autosampler, thermostated column oven and photodiodearray detector (PDA). Data were acquired and processed with ChemStation (Agilent, Palo Alto, CA, U.S.A.). A C-18 reversed-phase column (Zorbox Eclipse XDB-C18, 4.6 × 50 mm, 1.8 μm, Agilent) was used for the separation of ECD and DPs. An isocratic elution was achieved using a mobile phase which consisted of methanol and sodium acetate (pH 7.0, 50 mM; 60 : 40, v/v). The flow-rate was 0.5 mL/min and the injection volume was 2-5 μL. The absorbance detection wavelength was 210 nm. The column temperature was set at 25°C in all experiments performed.

2.3 LC-MS/MS and MS/TOF instrumentation

MS analysis was carried out on a 4000 QTrap LC-MS/MS system with API Analyst software of version 1.4.1 or a QSTAR Elite Hybrid QTOF with API Analyst QS software of version 2.0 (MDS Sciex, Ontario, Canada). Samples were introduced by an HPLC system (Agilent 1100 series HPLC system, Agilent, CA, U.S.A.) or a syringe pump (Harvard, Harvard Apparatus Inc., Holliston, MA, U.S.A.). The samples were ionized by a turbo spray ion source (electrospray ionization) in the positive ion mode at 5500 V. Mass spectra were obtained over the range of 50 or 100 to 2000 amu with unit resolution in Q1 and Q3. Other parameters are shown in Table 1. In all cases of 4000 QTrap LC-MS/MS studies, nitrogen was used as the nebulization, curtain and collision gas.

2.4 HPLC method development and validation

The method was validated according to the International Conference on Harmonization (ICH) guidelines for the validation of analytical methods, which includes specificity, linearity, precision, accuracy, LOD/LOQ, solution stability, robustness and system suitability and was achieved as the procedures described earlier (Liu et al., 2008; Yang et al., 2010).

2.4.1 Specificity (selectivity)

Forced degradation studies are used to evaluate the development of analytical methodology (the specificity or selectivity of the purity assay method), to gain better understanding of the stability of APIs and drug products and to provide information about degradation pathways and DPs.

Parameter	Q1 scan	MS2 scan	TOF MS
Source Type	Turbo Spray	Turbo Spray	Turbo Spray
Source Temperature (°C)	-	-	-
Scan Type	Q1 MS	Product Ion (MS2)	Positive TOF
Scan Mode	Profile	Profile	None
Polarity	Positive	Positive	Positive
Resolution (Q1 & Q3)	Unit	Unit	Unit
Nebulizer Gas (NEB)	-	-	-
Curtain Gas (CUR)	10	10	20
IonSpray Voltage (IS, V)	5500	5500	5500
Collision Gas (CAD)	-	Medium	-
Ion Source Gas 1 (GS1)	20	20	20
Ion Source Gas 2 (GS2)	0	0	0
Ion Energy 1 (IE1, V)	0.30	0.30	1.00
Ion Energy 3 (IE3, V)	-	-0.50	-
Detector Parameters	Positive	Positive	-
Deflector (DF)	-	-	-
Channel Electron Multiplier (CEM, V)	1950	1950	-

Table 1. Mass spectrometry working parameters for ECD and DPs analysis

Here, forced degradation studies of ECD were carried out under the conditions of acidic and alkaline hydrolysis, oxidation and dry heat. Samples of ECD (2 mg) were dissolved in 0.34 mL of methanol and subjected to 0.33 mL of 1 M HCl and 0.33 mL of 1 M NaOH at ambient temperature for 4 hrs and 1 hr, respectively. Acidic and alkaline hydrolysis samples were neutralized using 1 M NaOH or 1 M HCl and diluted to 2 mg/mL with methanol before HPLC analysis. Equivalent amounts (2 mg) of ECD that one portion was dissolved in 0.50 mL of methanol and subjected to 0.50 mL of 3% H_2O_2 and the other portion of solid drug was heated at 50°C (in oven over a period of 4 hrs) and were injected into the HPLC for analysis.

2.4.2 Linearity

The calibration curves of five concentrations (1.6 to 2.4 mg/mL) were obtained by plotting the respective peak areas against concentrations. The linearity was evaluated by the linear least square regression method with three determinations at each concentration.

2.4.3 Precision

In relation to the precision of the method, repeatability (intra-day), intermediate (inter-day) precision and reproducibility were investigated by performing assays of retention times, peak widths at half height, number of theoretical plates, linear least squares regression equations and correlation coefficients for the ECD standard at five concentrations and purities for one quality control (QC) sample. The repeatability and intermediate precision were evaluated by one analyst within one and two days, respectively, while the reproducibility was achieved by two analysts (Kulikov & Zinchenko, 2007).

2.4.4 Accuracy (recovery)

The accuracy of the method was determined by the recovery test. QC samples of ECD of concentration at 2.0 mg/mL ($C_{nominal}$) were analyzed by the proposed method. Experimental values (C_{exp}) were obtained by interpolation to the linear least square regression equation of a fresh newly prepared calibration curve (1.6 to 2.4 mg/mL) and comparing with the theoretical values ($C_{nominal}$).

$$\text{Recovery yield (\%)} = \frac{C_{exp}\,(\text{mg/mL})}{C_{nominal}\,(\text{mg/mL})} \times 100\%$$

2.4.5 Limit of detection (LOD) and limit of quantification (LOQ)

The LOD and LOQ of the method for impurities in ECD were determined at signal to noise ratios of 3 and 10, respectively.

2.4.6 Stability of drug (API) solution

The stability of the API solution was examined using the QC sample (2.0 mg/mL) for bench-top stability study. The QC samples were kept in the autosampler at ambient temperature for HPLC analysis over three consecutive days. Experimental data were obtained by interpolation to the linear least square regression equation of a calibration curve (1.6 to 2.4 mg/mL) newly prepared each day. Retention time, recovery yield and purity of ECD over three consecutive days were analyzed.

2.4.7 Robustness

The robustness of an analytical method is a basic measurement of its capacity to remain unaffected by small variations in method parameters. In this investigation, method robustness was evaluated through the effects of different columns (same type and manufacturer), column temperatures (± 2°C), pH values (± 0.1) and flow rates (± 0.05 mL/min) of mobile phase.

2.4.8 System suitability

The system suitability was assessed by five triplicate analyses of the drug in a concentration range of 1.6 to 2.4 mg/mL. The efficiency of the column was expressed in terms of the

theoretical plates number (N), column capacity (k'), column selectivity (α) and tailing factor (t). The acceptance criteria for the N, k', α, t and percentage relative standard deviation (% R.S.D.) for the retention time of ECD were > 3000, 2-8, 1.05-2.00, 0.9-2.5 and ± 2%, respectively.

2.5 Forced degradation studies of ECD

Forced degradation studies of ECD were carried out according to the procedures described above in Section 2.4.1 Specificity (selectivity). Moreover, samples of ECD (2 mg) were dissolved in 0.50 mL of methanol and subjected to 0.25 mL of 1 M NaOH and 0.50 mL of 3% H_2O_2 at ambient temperature for kinetic studies. The structures and degradation of DPs were further characterized by HPLC and LC-MS/MS for the molecular weights and the CAD fragmentation pathways.

2.6 Degradation studies of ECD Kit

First, degradation studies of ECD Kit were carried out by subjecting samples of ECD to various components of ECD Kit for determining the effect of $SnCl_2$, mannitol and EDTA. Second, ECD (1 mg/mL, 500 μL) and $SnCl_2$ (1 mg/mL) were mixed in ratio of 12.5 : 1, 8 : 1, 4 : 1, 2 : 1 and 1 : 1 (v/v) and diluted to total volume of 1000 μL with deionized water. The mixtures were kept at ambient temperature in HPLC autosampler and in bench-top for HPLC and MS analysis, respectively. All samples were diluted to 1 ppm with methanol for MS analysis. Positive ESI-MS/MS scanning types, i.e. precursor ion scan, product ion scan and neutral loss scan were performed. The structures of DPs were proposed based on the molecular weights and the CAD fragmentation pathways.

3. Results and discussion

3.1 HPLC method development

A reversed-phase high performance liquid chromatography (RP-HPLC) method for the determination of ECD and forced degradation DPs was developed and validated. A Zorbox Eclipse XDB-C18 (4.6 × 50 mm, 1.8 μm, Agilent) reversed-phase column was selected for the separation of ECD and DPs. ECD samples at concentrations of around 2 mg/mL and 100 ppb were used to optimize conditions for HPLC and LC-ESI-MS/MS, respectively. Absorption spectra of ECD were recorded over the range of 200 to 300 nm by a post-column photodiode-array detector (PDA). A wavelength of 210 nm was found to be optimal for the detection and quantification of ECD.

Chromatographic separation of ECD was achieved using a mobile phase which consisted of methanol and sodium acetate (pH 7.0, 50 mM; 60 : 40, v/v). The typical HPLC chromatograms of ECD are shown in Fig. 3(a) and 4(a). The difference of retention time (t_R) of ECD chromatograms between degradation studies of API and drug product was due to the gradual damage of column packing materials. However, no significant efficiency of the column, such as the number of theoretical plates (N) and tailing factor (t) was found.

3.2 Mass spectrometric analysis of ECD

The proposed high-salt contained mobile phase of HPLC was not suitable for ESI-MS studies. Therefore, a syringe pump was chosen for the sample introduction for Q1 and MS/MS scan. Q1 full scans were achieved in a positive ion mode to optimize the

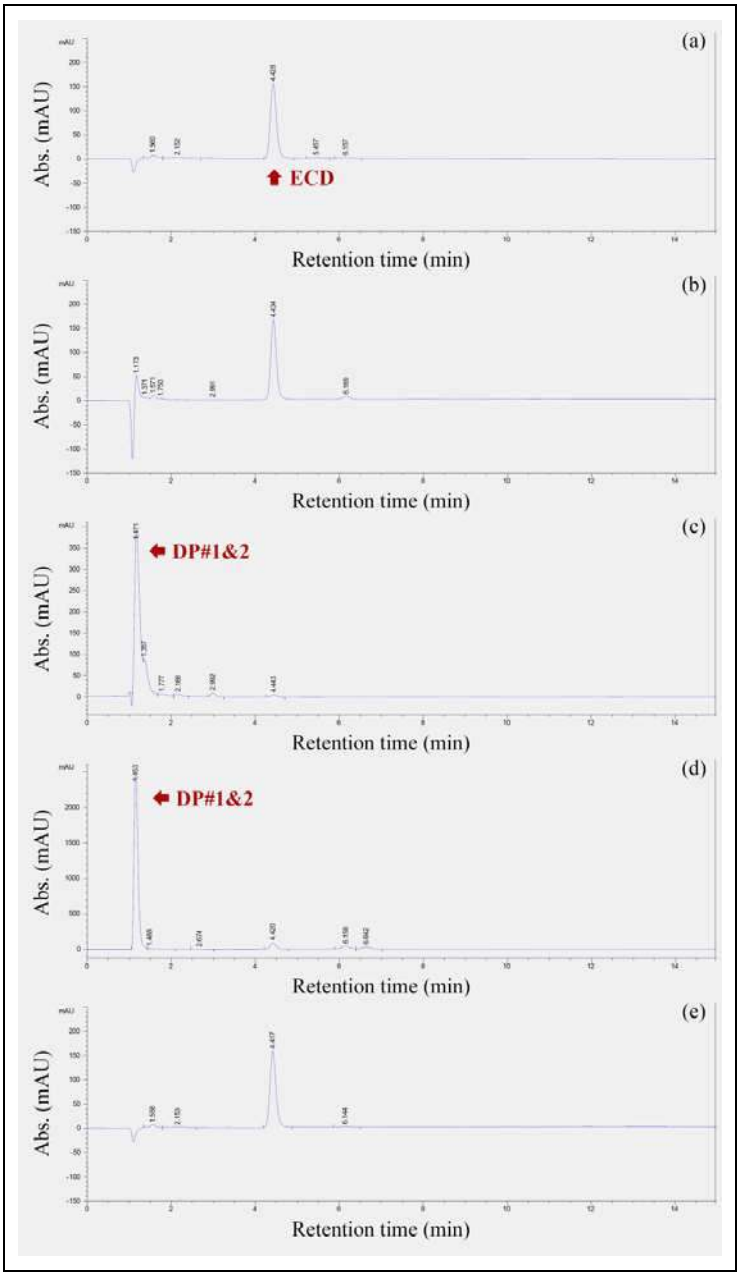

Fig. 3. Typical HPLC chromatograms of degradation studies of ECD. Samples (2 mg of ECD) were carried out under the conditions of (a) methanol (no degradation), (b) acidic hydrolysis (0.5 M HCl at ambient temperature for 4 hrs), (c) alkaline hydrolysis (0.5 M NaOH at ambient temperature for 1 hr), (d) oxidation (1.5% H_2O_2) and (e) dry heat (50°C for 4 hrs)

electrospray ionization (ESI) conditions of ECD and $(ECD)_2$ (Fig. 5(a)). The peaks at retention time (t_R) of 4.43 and 3.82 min were identified as a protonated ECD ion ($[M+H]^+$) at m/z 323.4 by ESI-MS (Fig. 5(b)). Moreover, a protonated molecular ion with m/z 645.4 at t_R of 6.17 and 5.27 min were identified as ECD dimer (DP#3), i.e. $(ECD)_2$ (Fig. 5(g)).

Both product ion and precursor ion scans were then carried out at different collision-activated dissociation (CAD) conditions to optimize the declustering potential (DP), entrance potential (EP), collision energy (CE) and collision cell exit potential (CXP). The MS/MS fragments of ECD, ECD and $ECD_{S\text{-}S}$ are summarized in Table 2.

The linearities of multiple reaction monitoring (MRM) transitions of ECD ($ECD_{S\text{-}S}$) were studied. The linear least-square regression equations and correlation coefficients of MRM transitions showed a good linearity over the calibration range. The correlation coefficients (r) were all above 0.9980, indicating the stability of these fragmentations (data not shown). Tandem mass spectrometry (MS/MS) experiments performed in a QTrap MS were used to investigate the CAD fragmentation behavior of ECD ($ECD_{S\text{-}S}$) (Fig. 6(a)).

Although precursor scan of m/z 323.50 can show its precursor ion at m/z 325.40 and 646.36, we found that intra-molecular disulfide product ($ECD_{S\text{-}S}$) is the prominent form in aqueous solution than ECD. This is consistent with previous experiment by Verduyckt et al. (2003), in which they pointed out the existence of disulfide and incomplete esterification of ethylene dicysteine derivatives.

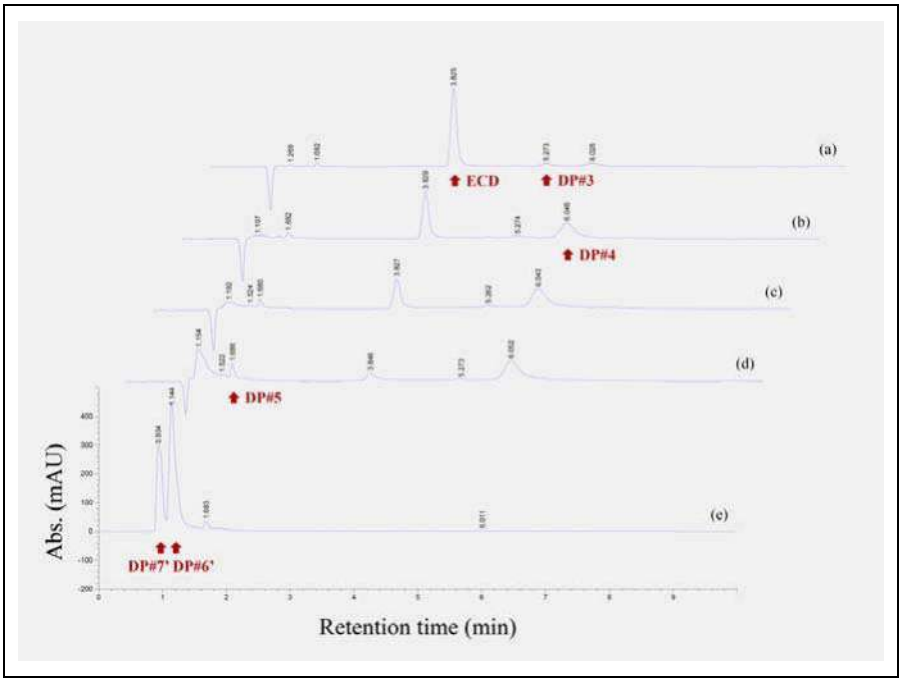

Fig. 4. Typical HPLC chromatograms of degradation studies of ECD Kit. Samples were carried out by subjecting ECD to $SnCl_2$ in ratio (v/v) of (a) 1 : 0, (b) 12.5 : 1, (c) 8 : 1, (d) 4 : 1 and (e) 2 : 1. Duration time is 7-8 hrs

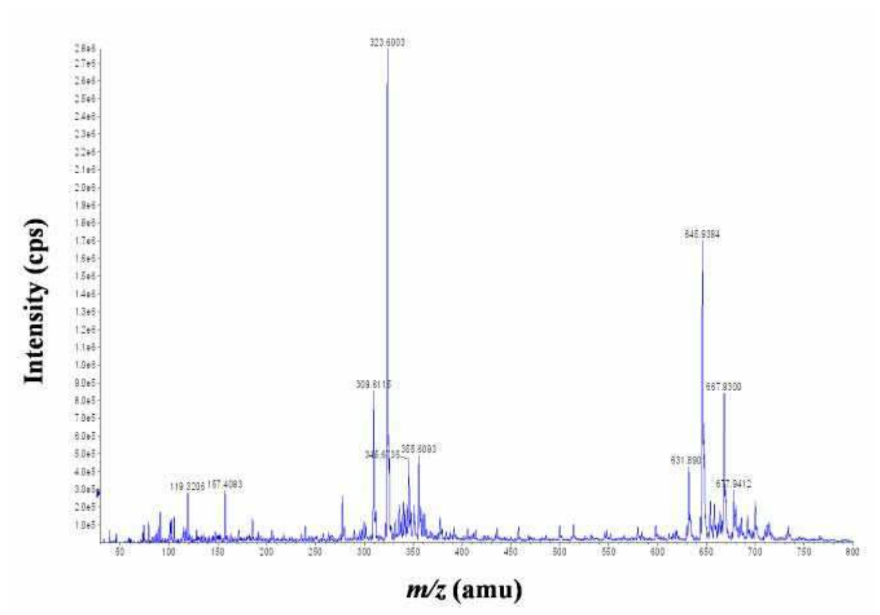
Intensity (cps)
m/z (amu)
323.6003
646.9384
309.6115
667.8300
631.890
119.3206
157.4083

(a)

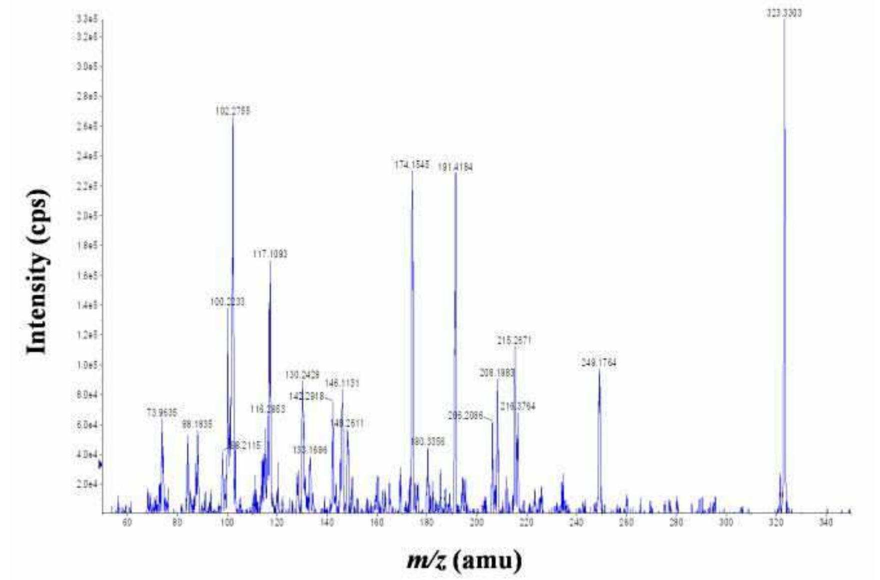
Intensity (cps)
m/z (amu)
323.3303
102.2768
174.1548
191.4184
117.1093
215.2871
249.1764
73.9635

(b)

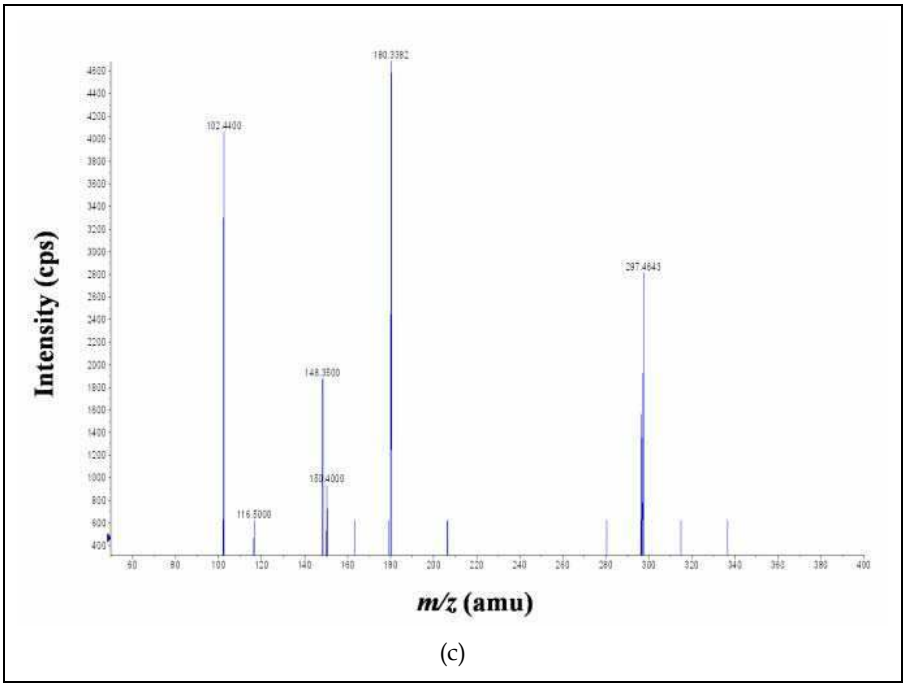
Intensity (cps)
m/z (amu)
180.3382
102.4400
297.4643
148.3500
159.4000
116.5000

(c)

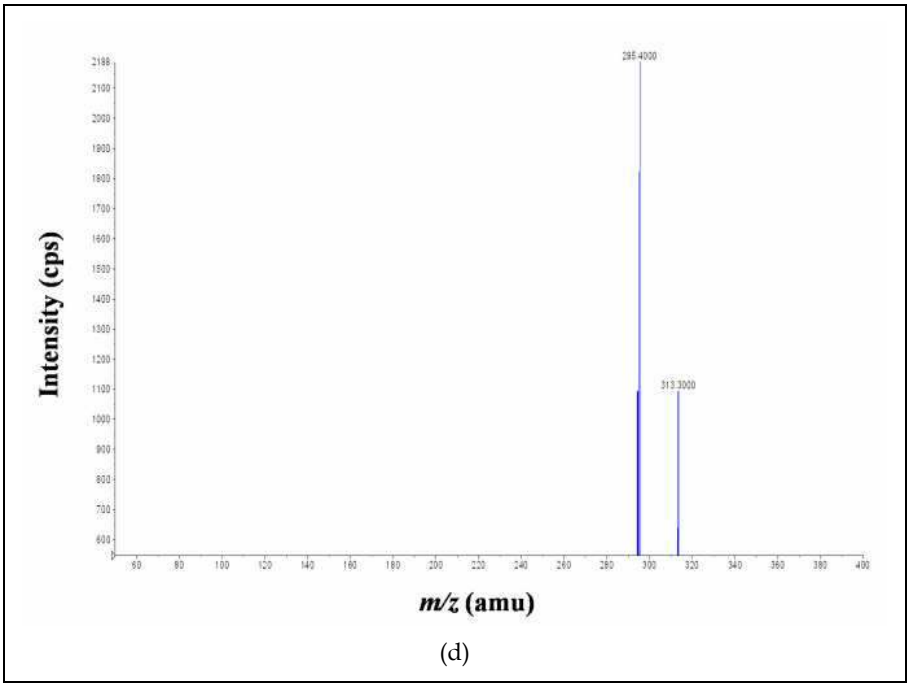
Intensity (cps)
m/z (amu)
295.4000
313.3000

(d)

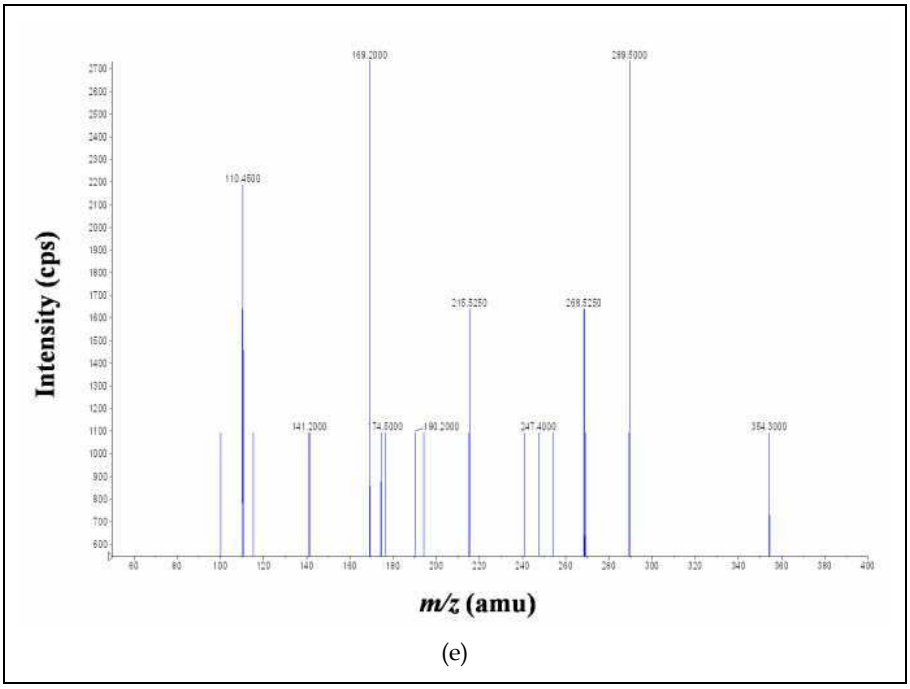
Intensity (cps)
m/z (amu)
169.2000
289.5000
110.4600
216.5250
268.5250
141.2000
74.5000
190.2000
247.4000
364.3000

(e)

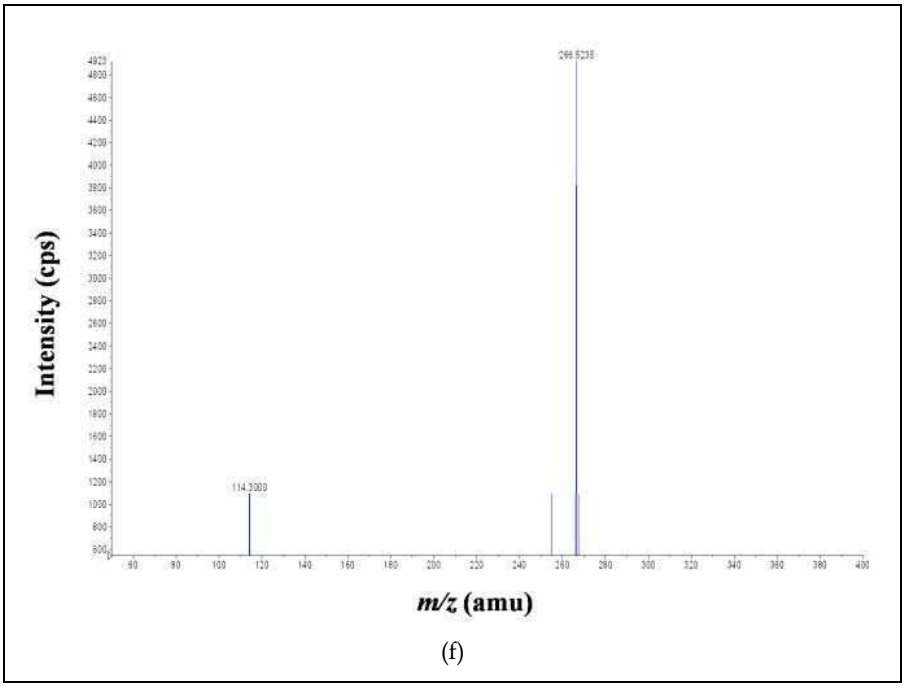
Intensity (cps)
m/z (amu)
289.5238
114.3000

(f)

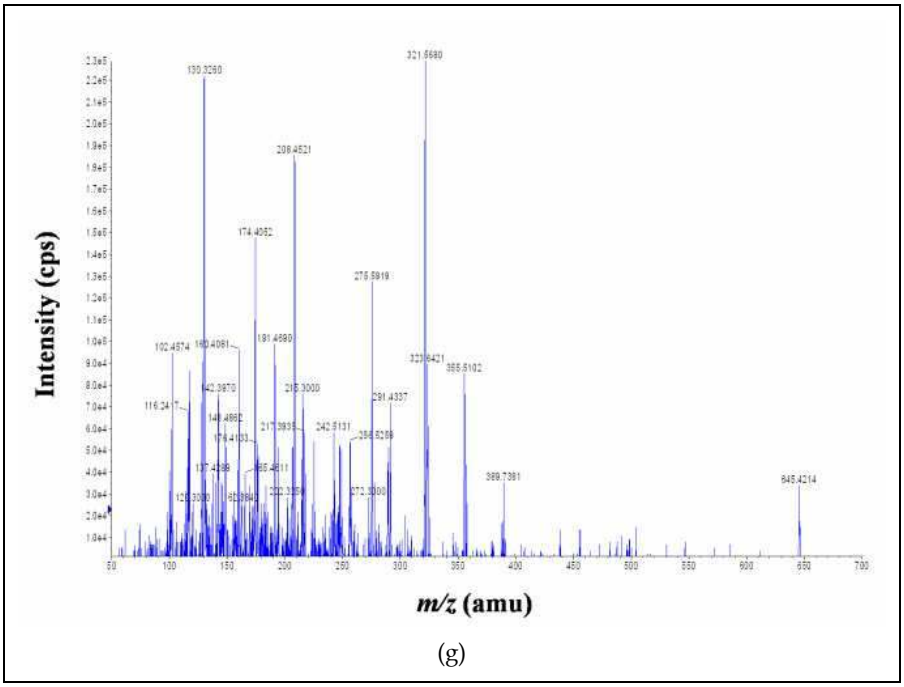
Intensity (cps)
m/z (amu)
321.5680
130.3260
208.4521
174.4062
276.5919
102.4574
160.4081
181.4690
323.6421
355.5102
116.2417
142.3970
216.3000
291.4337
242.5131
389.7381
845.4214

(g)

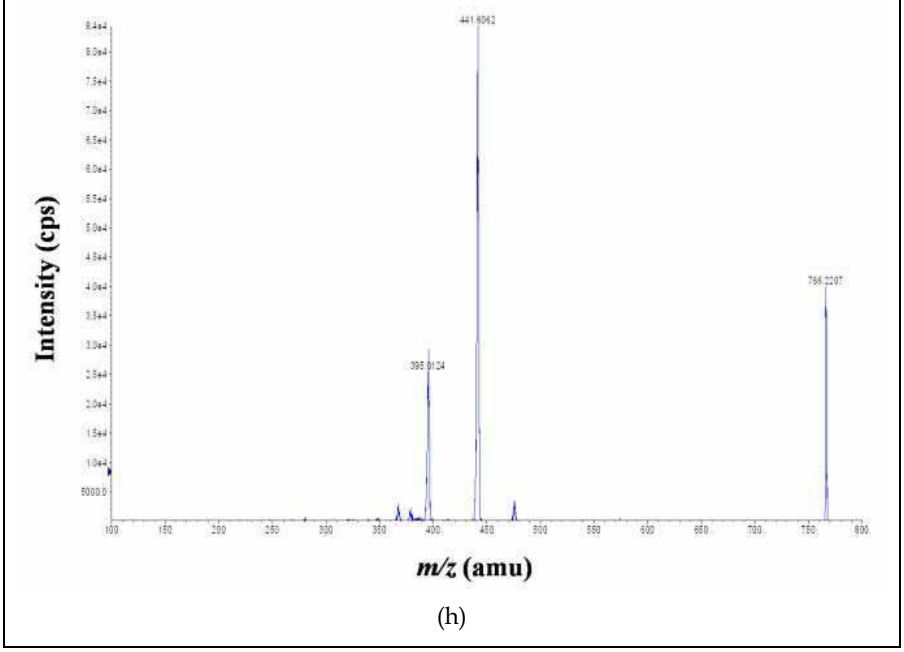
Intensity (cps)
m/z (amu)
441.6062
766.2207
398.6124

(h)

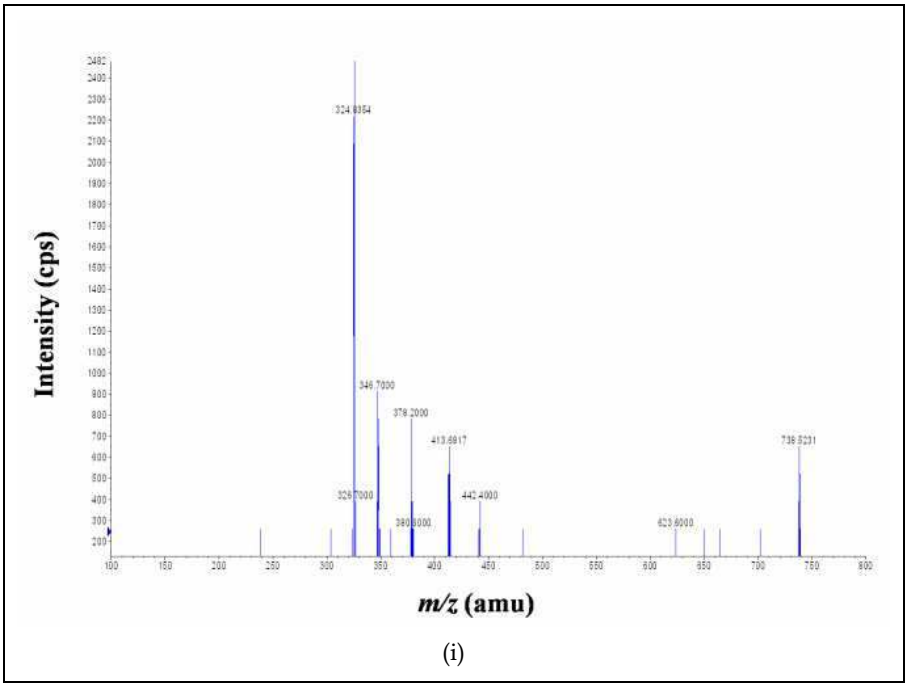
Intensity (cps)
m/z (amu)
324.8354
346.7000
378.2000
413.6917
442.4000
326.7000
380.8000
623.6000
738.8231

(i)

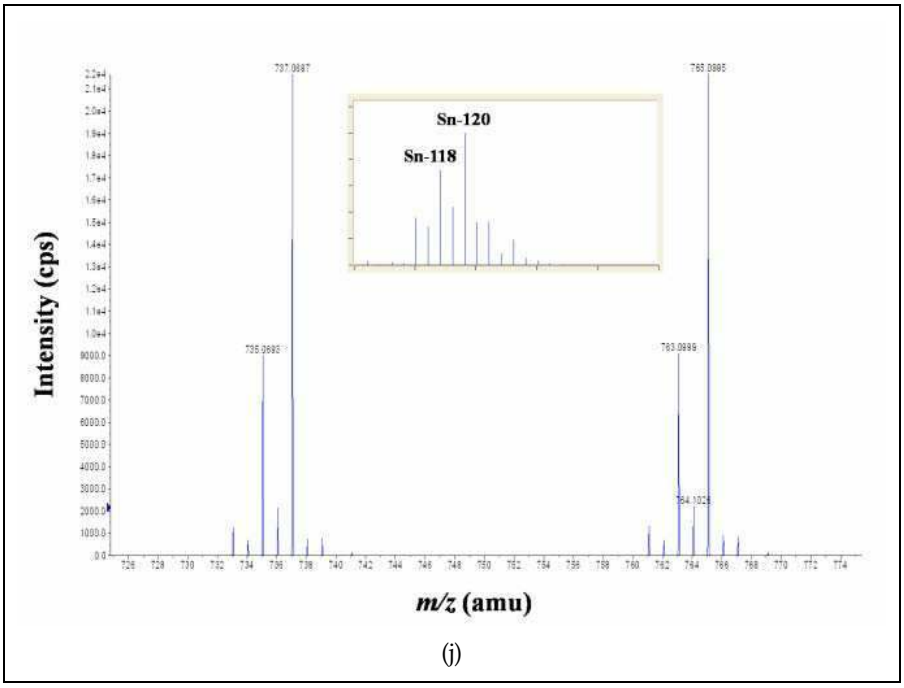
Intensity (cps)
m/z (amu)
737.0697
783.0895
735.0693
783.0899
Sn-120
Sn-118

(j)

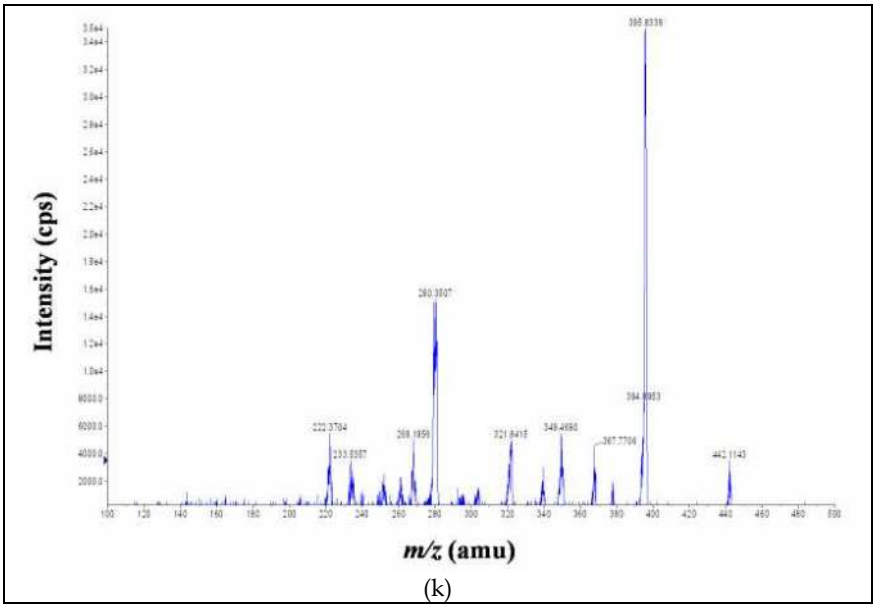

(k)

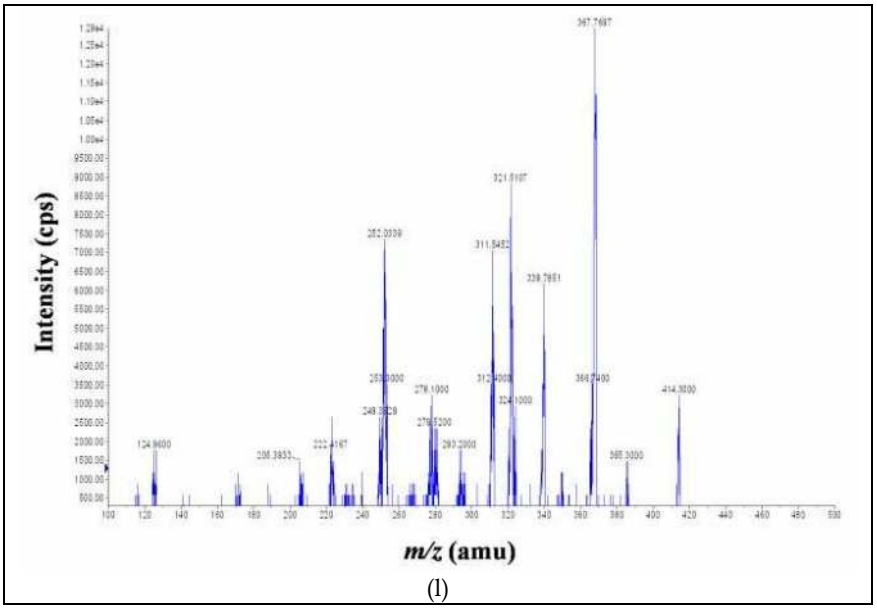

(l)

Fig. 5. (a) Typical ESI-MS Q1 spectra of ECD, typical ESI-MS/MS product ion spectra of (b) $ECD_{S\text{-}S}$ (m/z 323.4), (c) DP#1 (ECD-Et, m/z 297.5), (d) DP#1′ ($(ECD)_{S2N2}$-Et, m/z 295.4), (e) DP#2 (ECD-2Et, m/z 268.5), (f) DP#2′ ($(ECD)_{S2N2}$-2Et, m/z 266.5), (g) DP#3 ($(ECD)_2$, m/z 645.4), (h) DP#4 ($Sn(ECD)_2$, m/z 766.4), (i) DP#5 ($Sn(ECD)_2$-Et, m/z 738.0), (j) isotopic ESI-TOF spectra of DP#4 ($Sn(ECD)_2$) and DP#5 ($Sn(ECD)_2$-Et), (k) DP#6′ ($Sn(ECD)_{S2N2}$, m/z 442.0) and (l) DP#7′ ($Sn(ECD)_{S2N2}$-Et, m/z 414.0)

ECD and DPs		Molecular Formula	mw_{avg} or mw_{max}†	Major fragments (m/z)
	ECD	$C_{12}H_{24}N_2O_4S_2$	324.46	175.72, 147.79, 132.53, 129.30, 119.47, 101.52, 86.53
	$ECD_{S\text{-}S}$	$C_{12}H_{22}N_2O_4S_2$	322.45	323.33, 249.18, 215.27, 208.20, 191.42, 174.15, 146.11, 130.24, 117.11, 102.28, 88.18, 73.96
DP#1	ECD-Et	$C_{10}H_{20}N_2O_4S_2$	296.41	297.46, 180.34, 148.35, 102.44, 74.30
DP#1′	$ECD_{S\text{-}S}$-Et	$C_{10}H_{18}N_2O_4S_2$	294.39	295.40, 313.30, 248.40, 219.20, 139.50, 117.40
DP#2	ECD-2Et	$C_8H_{16}N_2O_4S_2$	268.36	268.53, 289.50, 354.30, (322.40, 304.53), 247.40, 215.52, 190.20, 169.20, 110.45
DP#2′	$ECD_{S\text{-}S}$-2Et	$C_8H_{14}N_2O_4S_2$	266.34	266.52, 114.30
DP#3	$(ECD)_2$	$C_{24}H_{44}N_4O_8S_4$	644.90	389.74, 355.51, 321.57, 275.59, 215.3, 208.45, 191.47, 174.41, 130.33, 116.24, 102.46
DP#4	$Sn(ECD)_2$	$C_{24}H_{44}N_4O_8S_4Sn$	764.80†	441.61, 396.01, 367.20, 321.40, 280.40
DP#5	$Sn(ECD)_2$-Et	$C_{22}H_{40}N_4O_8S_4Sn$	736.74†	442.40, 413.69, 378.20, 346.70, 324.84
DP#6′	$Sn(ECD)_{S2N2}$	$C_{12}H_{20}N_2O_4S_2Sn$	440.33†	395.83, 367.77, 349.47, 321.84, 280.35, 268.20, 222.37
DP#7′	$Sn(ECD)_{S2N2}$-Et	$C_{10}H_{16}N_2O_4S_2Sn$	412.28†	385.30, 367.77, 339.79, 321.51, 311.55, 293.20, 279.52, 278.10, 252.03, 222.42, 205.38, 124.96

Table 2. Major MS/MS fragments of ECD and DPs. †mw_{max}: Theoretic molecular weight of maximum isotopic composition

3.3 HPLC method validation

3.3.1 Specificity (selectivity)

ECD was firstly subjected to forced degradation under the conditions of hydrolysis (acid, alkali and neutral), oxidation and thermal stress as requirements of ICH. Significant degradations of 0.5 M NaOH and 1.5% hydrogen peroxide were noticed under stress conditions. Several DPs in the chromatograms at the t_R of 6.64, 2.99, 2.17 and 1.00-1.50 min were detected as shown in Fig. 3(c) and 3(d). Fig. 3(b) and 3(e) represent the chromatograms of a sample degraded at 0.5 M HCl and 50°C for 4 hrs, respectively. No significant degradation was found in these cases. The resolutions between ECD and its degradation peaks were greater than 4.4, indicating that the proposed method was sufficiently selective for its intended purpose.

3.3.2 Linearity

Standard curves were constructed by plotting peak area against concentration of ECD and were linear over the concentration range of 1.6 to 2.4 mg/mL. The linear least squares regression equation of the standard curve correlating the peak areas (PAs) to the drug

concentration (X in mg/mL) in this range was Y = 832.03X - 148.88. The correlation coefficient (r) was 0.9991.

3.3.3 Precision

The results of repeatability, intermediate precision and reproducibility were demonstrated by analysing ECD at five concentrations and one QC sample (Table 3). Although the number of theoretical plates were decreased for ~20%, no significant difference in the retention times, peak widths at half height, linear least squares regression equations and correlation coefficients were found. The difference of purities (P (%)) could be due to the stability (equilibrium) and uniformity of QC samples, but also might indicate the sufficient resolution of the proposed method.

Parameters	t_R (min)	W_{half} (min)†	N†	L eq.†	r	P (%)‡
Analyst 1, Day 1	4.42 ± 0.00 (0.05%)	0.15 ± 0.00 (1.27%)	5007 ± 129 (2.58%)	Y = 859.35X - 204.71	0.9998	100.30 ± 0.01
Analyst 1, Day 2	4.42 ± 0.00 (0.06%)	0.15 ± 0.00 (0.69%)	4933 ± 66 (1.34%)	Y = 910.18X - 244.25	0.9992	99.20 ± 0.02
Analyst 2, Day 3	4.41 ± 0.00 (0.05%)	0.16 ± 0.00 (0.81%)	4174 ± 67 (1.61%)	Y = 834.46X - 127.08	0.9990	97.42 ± 0.00

Table 3. Repeatability, intermediate precision and reproducibility of ECD analysis. †Linear range: 1.6 to 2.4 mg/mL; W_{half}: Peak width at half height; N: Number of theoretical plates; n = 15. ‡P (%): The purity of QC sample (n = 3)

3.3.4 Accuracy (recovery)

Recovery tests were achieved by comparing the concentration (C_{exp}) obtained from injection of QC samples to the nominal values ($C_{nominal}$). The intra-day recovery of ECD at concentration of 1.95 mg/mL was 99.68 ± 0.48%. The recoveries, 99.14, 99.89 and 100.03% were between 97 and 103%, indicating that there was sufficient accuracy in the proposed method. The % R.S.D. for measurement of accuracy was 0.48%.

3.3.5 Limit of detection (LOD) and limit of quantification (LOQ)

The limits of detection (LOD, S/N = 3/1) and quantification (LOQ, S/N = 10/1) for the major impurity (DP#3, average abundance in percentage of peak area = 1.32 ± 0.07%) in ECD were found to be 0.004 and 0.014 mg/mL (n = 3), respectively.

3.3.6 Stability of drug (API) solution

The stability of ECD solutions was examined by analyzing solutions over 3 days. The results of these studies are shown in Table 4, where the t_R of ECD and the recovery and purity of QC samples were within the range of 97-103%. No significant degradation or reduction in the absolute peak area was observed within three days, indicating that ECD standard solution would be stable for at least three days when kept on a bench top.

3.3.7 Robustness

The robustness of an analytical procedure is a measurement of its capacity to remain unaffected by small, but deliberate, variations in method parameters and provides an

indication of its reliability during normal usage. In this case, robustness of the method was investigated by making small changes of column parameters, column temperature, mobile phase pH and flow rate. The results of the robustness studies were within acceptable range, except that one theoretical plates number (N) was less than 3000, as indicated in Table 5. However, no critical change in performance was found.

Day	Calibration range (mg/mL)	L eq.	r	t_R (min)†	P (%)†
1	1.51-2.33	Y = 859.35X - 204.71	0.9998	4.42 ± 0.00 (0.05%)	100.30 ± 0.97 (0.97%)
2	1.58-2.44	Y = 910.18X - 244.25	0.9992	4.42 ± 0.00 (0.06%)	99.66 ± 1.07 (1.08%)
3	1.54-2.36	Y = 834.02X - 114.17	0.9948	4.40 ± 0.00 (0.04%)	100.13 ± 1.14 (1.14%)

Table 4. Bench-top stability studies of ECD. †The retention time and purity results of QC samples (n = 3)

Parameters		t_R (min)	W_{half} (min)	N	L eq.	R	P (%)*
Column†	#1	4.49 ± 0.00 (0.05%)	0.19 ± 0.00 (1.46%)	n. r.#	Y = 842.24X - 138.39	0.9984	98.99 ± 0.12
	#2	4.42 ± 0.00 (0.05%)	0.15 ± 0.00 (1.27%)	5007 ± 129 (2.58%)	Y = 859.35X - 204.71	0.9998	100.30 ± 0.97
Temperature (°C)	25	4.41 ± 0.00 (0.05%)	0.16 ± 0.00 (0.81%)	4174 ± 67 (1.61%)	Y = 834.46X - 127.08	0.9990	97.42 ± 0.28
	27	4.35 ± 0.00 (0.07%)	0.17 ± 0.00 (1.83%)	3698 ± 138 (3.74%)	Y = 849.90X - 154.71	0.9996	97.13 ± 0.22
pH‡	6.9	4.41 ± 0.00 (0.08%)	0.14 ± 0.00 (0.75%)	5418 ± 84 (1.55%)	Y = 860.08X - 227.29	0.9983	99.21 ± 0.87
	7.0	4.42 ± 0.00 (0.05%)	0.15 ± 0.00 (1.27%)	5007 ± 129 (2.58%)	Y = 859.35X - 204.71	0.9998	100.30 ± 0.97
	7.1	4.40 ± 0.00 (0.09%)	0.15 ± 0.01 (5.11%)	4777 ± 465 (9.73%)	Y = 900.62X - 270.33	0.9968	99.90 ± 0.06
Flow rate (mL/min)	0.45	5.00 ± 0.00 (0.06%)	0.25 ± 0.00 (0.92%)	2249 ± 43 (1.90%)	Y = 986.87X - 253.74	0.9967	100.69 ± 0.43
	0.50	4.49 ± 0.00 (0.05%)	0.19 ± 0.00 (1.46%)	n. r.#	Y = 842.24X - 138.39	0.9984	98.99 ± 0.12
	0.55	4.08 ± 0.00 (0.10%)	0.18 ± 0.00 (1.77%)	n. r.#	Y = 808.35X - 177.83	0.9981	98.75 ± 0.18

Table 5. Robustness study of ECD calibration standard and QC samples analysis. †Column #1 and #2 refer to columns of same type, same manufacturer, but different batch. ‡The pH value of the original aqueous component. *P (%): The purity of QC sample. #n. r.: No record

3.3.8 System suitability

The theoretical plates number (N), column capacity (k'), column selectivity (α) and tailing factor (t) were 5007 ± 129 (2.58%), 2.85 ± 0.01 (0.18%), 1.31 ± 0.00 (0.00%) and 1.19 ± 0.01 (1.07%), respectively. The repeatabilities (% R.S.D.) of t_R for triplicate analysis were within the acceptance criterion range (± 2%). These results were within acceptable range.

3.4 Forced degradation studies of ECD

ECD was subjected to forced degradation under the conditions of hydrolysis (acid, alkali and neutral), oxidation and thermal stress as requirements of ICH. No significant

degradation product under the stress conditions of neutral solvents, acidic hydrolysis and dry heat was found (Fig. 3(a), 3(b) and 3(e)). On the contrary, the drug was demonstrated to be liable to degradation under the alkaline hydrolysis and oxidation stress conditions. The reaction in 0.5 M NaOH and 1.5% H_2O_2 at ambient temperature was so fast that almost 100% of ECD was degraded within 1 hr and even immediately, respectively (Fig. 3(c) and 3(d)).

Several high polarity degradants of alkaline hydrolysis of esters in ECD, i.e. DP#1, DP#1′, DP#2 and DP#2′ were formed. The MS/MS spectra are presented in Fig. 5(c)-5(f) and the major fragments are summarized in Table 2. DP#1 and DP#1′ were shown to be monoacid monoester degradants of ECD and $ECD_{S\text{-}S}$, whereas DP#2 and DP#2′ were diacid degradants of ECD and $ECD_{S\text{-}S}$. These results are consistent with previous study (Verduyckt et al., 2003). The proposed structures of DP#1, DP#1′, DP#2 and DP#2′ are shown in Fig. 1

Under oxidation condition of 1.5% H_2O_2, our results also demonstrated that: (i) MS/MS fragments of DP#1, DP#1′, DP#2 and DP#2′ can be detected within duration time less than 0.5 hr, (ii) peak at t_R of 0.97 min was a mixture of DP#1, DP#1′, DP#2 and DP#2′ and (iii) MS/MS intensities of DP#2 and DP#2′ were significantly weaker than those of DP#1 and DP#1′.

Fragmentation ions at m/z 354.50, 322.40 and 304.53 (Table 2) can be detected in the precursor scan of DP#2 (mw_{avg} = 268.36) when the duration time was increased to 1.0 hr, indicating that further oxidation might result in dimer formation.

No protonated molecular ions of DP#1, DP#1′, DP#2 and DP#2′ were detected when $SnCl_2$ was added to the ECD aqueous solution, suggesting that concentrations of DP#1, DP#1′, DP#2 and DP#2′ were negligible in ECD Kit.

Comparing to the degradation rate under oxidation condition, alkaline hydrolysis was much more complicate, and several degradation intermediates were found before they were degraded to DP#1, DP#1′, DP#2 and DP#2′ (Fig. 3(c)).

3.5 Degradation studies of ECD Kit

ECD was very stable in deionized water, methanol and DMSO. The purity of ECD was kept in 95% for 45 hours, whereas ECD Kit was very unstable for quick deceasing to purity of 74.80% within 11 minutes.

ECD was subjected to various components of ECD Kit, such as $SnCl_2$, mannitol and EDTA, to investigate its degradation behavior. Bi-component mixtures of ECD and mannitol, EDTA and $SnCl_2$ in variant of ratio and duration time were analyzed by HPLC, MS and MS/MS.

Our preliminary results showed that mannitol and EDTA had no significant degradation effect in ECD and thus did not affect the purity of ECD. In contract to mannitol and EDTA, a positive correlation between ECD degradation and stannous chloride ($SnCl_2$) was found, suggesting that ECD degradation is significantly correlative to the ratio of ECD to $SnCl_2$ and duration time. These results demonstrated that $SnCl_2$ was the leading cause (key factor) for ECD degradation in ECD Kit. Therefore we prepared mixtures of ECD (1 mg/mL, 500 μL) and $SnCl_2$ (1 mg/mL) in ratio of 12.5 : 1 (the ratio of ECD to $SnCl_2$ in ECD Kit), 8 : 1, 4 : 1, 2 : 1 and 1 : 1 (v/v) and diluted to total volume of 1000 μL with deionized water. The mixtures were kept at ambient temperature in HPLC autosampler and in bench-top for HPLC and MS analysis, respectively.

Six major DPs of ECD, i.e. DP#3 - DP#7′ were numbered in sequence of the coordination number of ECD with Sn and hydrolysis of ester group in ECD. Their MS/MS spectra are

shown in Fig. 5(g)-5(l). These results did not quantify the effects on $SnCl_2$ on ECD degradation in detail due to the fact that the liability of $SnCl_2$ for oxidation in aqueous from Sn(II) to Sn(IV) make it difficult to exactly control the concentration of $SnCl_2$.

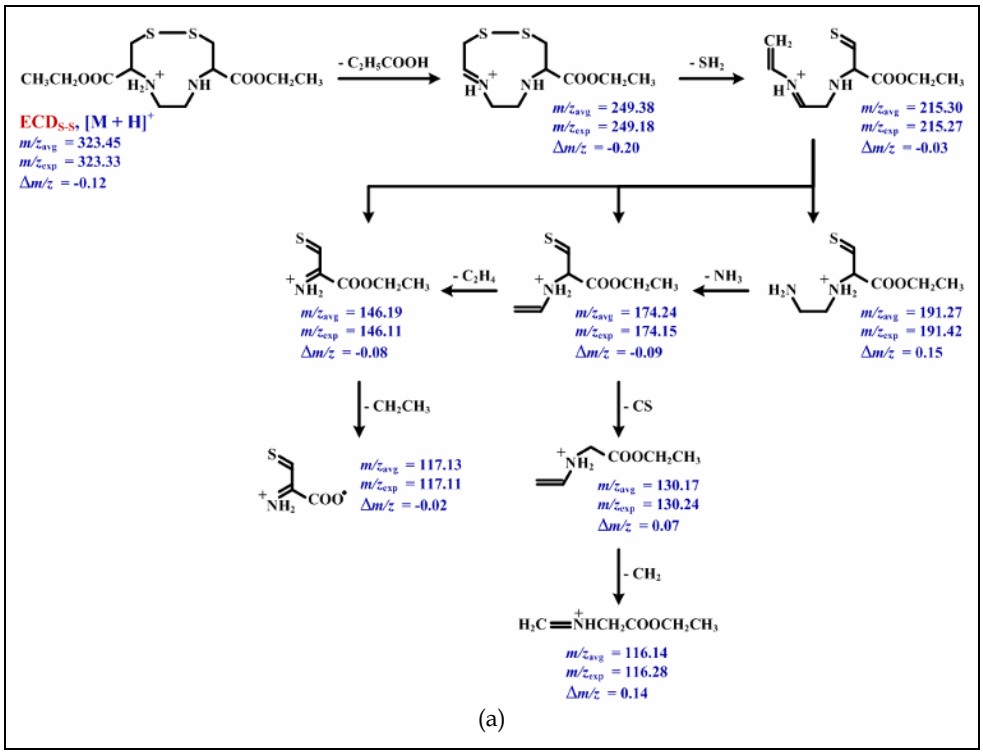

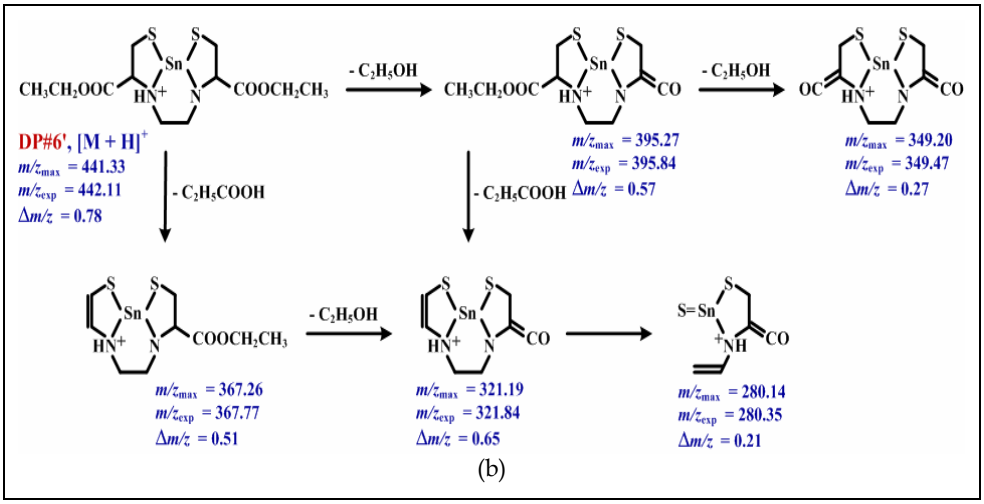

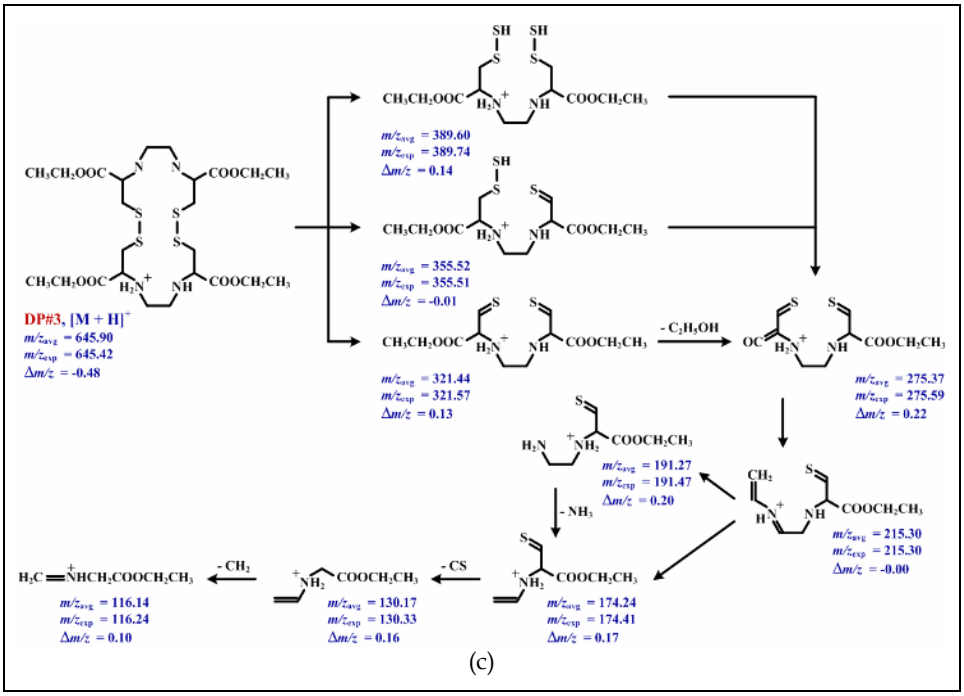
DP#3, [M + H]+
m/zavg = 645.90
m/zexp = 645.42
Δm/z = -0.48
m/zavg = 389.60
m/zexp = 389.74
Δm/z = 0.14
m/zavg = 355.52
m/zexp = 355.51
Δm/z = -0.01
m/zavg = 321.44
m/zexp = 321.57
Δm/z = 0.13
- C2H5OH
m/zavg = 275.37
m/zexp = 275.59
Δm/z = 0.22
m/zavg = 191.27
m/zexp = 191.47
Δm/z = 0.20
- NH3
m/zavg = 215.30
m/zexp = 215.30
Δm/z = -0.00
m/zavg = 174.24
m/zexp = 174.41
Δm/z = 0.17
- CS
m/zavg = 130.17
m/zexp = 130.33
Δm/z = 0.16
- CH2
m/zavg = 116.14
m/zexp = 116.24
Δm/z = 0.10

(c)

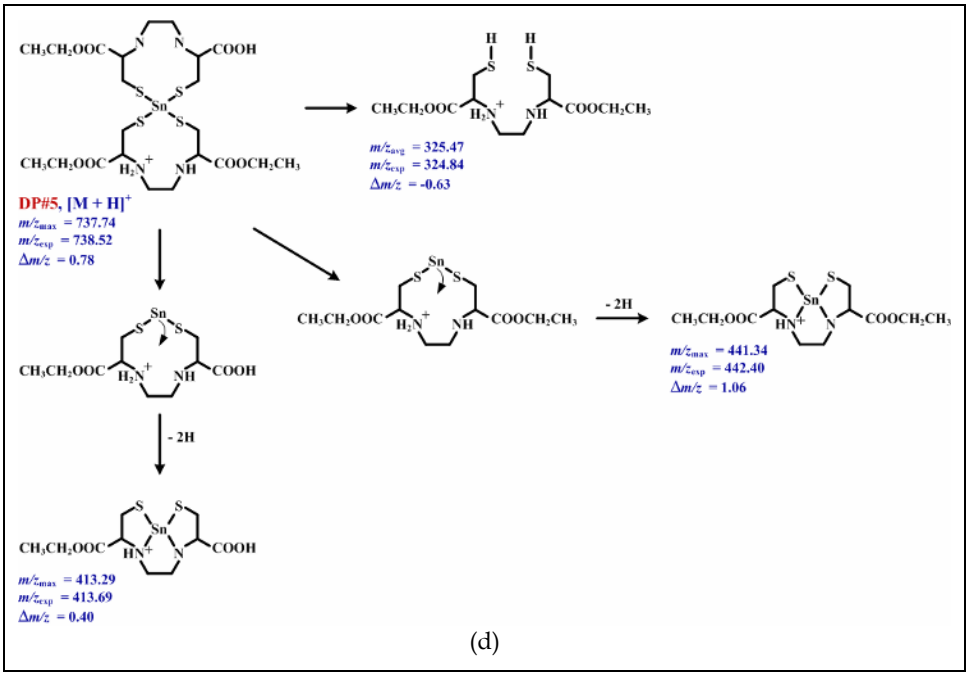
DP#5, [M + H]+
m/zmax = 737.74
m/zexp = 738.52
Δm/z = 0.78
m/zavg = 325.47
m/zexp = 324.84
Δm/z = -0.63
- 2H
m/zmax = 441.34
m/zexp = 442.40
Δm/z = 1.06
- 2H
m/zmax = 413.29
m/zexp = 413.69
Δm/z = 0.40

(d)

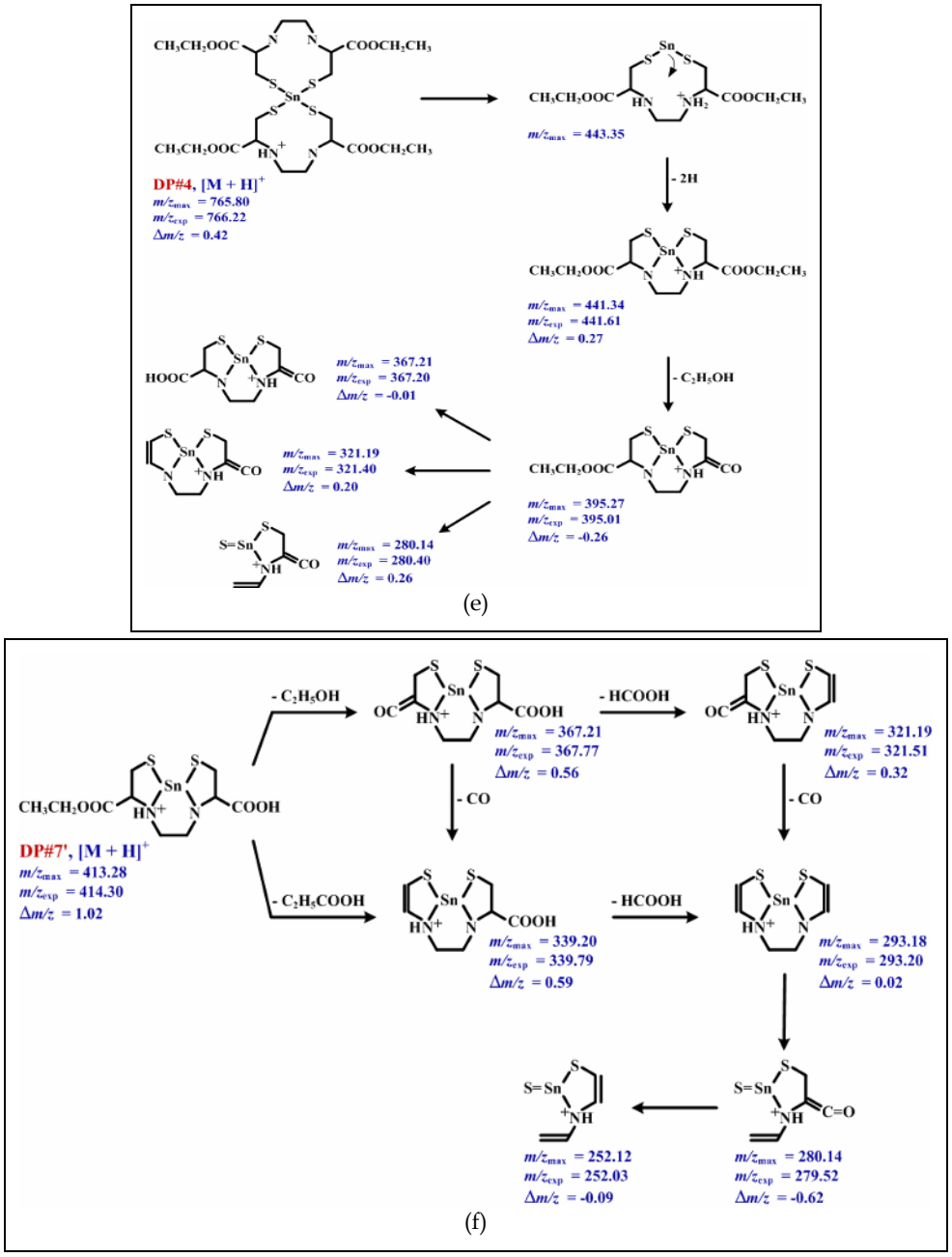

Fig. 6. Proposed CAD fragmentation pathways of the protonated molecules of (a) $ECD_{S\text{-}S}$ (m/z = 323.4), (b) $Sn(ECD)_{S2N2}$ (m/z = 442.0), (c) $(ECD)_2$ (m/z = 645.4), (d) $Sn(ECD)_2$-Et (m/z = 738.0), (e) $Sn(ECD)_2$ (m/z = 766.4) and (f) $Sn(ECD)_{S2N2}$-Et (m/z = 414.0)

3.5.1 Degradation product, DP#3

Here, we have identified the degradation production with intermolecular disulfide bond as (ECD_2), i.e. DP#3. The structure of DP#3 is shown in Fig. 1. In the HPLC chromatograms, DP#3 was found in the neutral solvents, acidic hydrolysis, oxidation, thermal degradation (Fig. 3 and 4(a)) and solutions with low concentration of $SnCl_2$ (Fig. 4(b) and (c)).

The typical product ion (MS/MS) scan spectra of protonated molecular ion with *m/z* 645.4 were identified as DP#3 (Fig. 5(g)). The MS/MS fragments of DP#3 are summarized in Table 2 and the linearities of MRM transitions were studied. The linear least-square regression equations and correlation coefficients ($r > 0.9990$) of MRM transitions showed a good linearity over the calibration range, indicating the stability of these fragmentations (data not shown).

Proposed CAD fragmentation pathways of the protonated molecules of DP#3 at m/z = 645.4 is presented in Fig. 6(c).

No significant hydrolysis product of DP#3, i.e. $(ECD)_2$-Et, $(ECD)_2$-2Et, $(ECD)_2$-3Et or $(ECD)_2$-4Et was detected in the MS scanning. Because species exchange reaction among ECD, ECD_{S-S} and $(ECD)_2$ was found in the HPLC chromatograms, we suggested that DP#3, $(ECD)_2$ can decompose reversibly into ECD or ECD_{S-S} and degrade further.

3.5.2 Degradation products, DP#4 and DP#5

In the ECD to $SnCl_2$ ratio of 12.5 : 1, 8 : 1 and 4 : 1 (v/v), one more nonpolar product (DP#4, t_R = 6.04 min) when compared to ECD and its polar hydrolysis product (DP#5, t_R = 1.68 min) were formed as indicated in Fig. 4(a)-(d). For higher concentration of $SnCl_2$ (ratio = 2 : 1 and 1 : 1), DP#4 was fast degraded and disappeared. The structures of DP#4 and DP#5 are shown in Fig. 1. The typical product ion (MS/MS) scan spectra of protonated molecular ions of DP#4 and DP#5 are shown in Fig. 5(h)-5(j). The MS/MS fragments of DP#4 and DP#5 are summarized in Table 2. Proposed CAD fragmentation pathways of the protonated molecules of DP#4 and DP#5 are shown in Fig. 6(e) and 6(d), respectively.

The peaks that appeared in the protonated molecular ions with the m/z range of 732 to 770 was further studied by TOF (Fig. 5(j)), the pattern was mainly due to the contribution of stable isotopes of tin and sulfur. Simulation spectra of DP#4 ($Sn(ECD)_2$) and DP#5 ($Sn(ECD)_2$-Et) are shown in the inset of Fig. 5(j). The isotopic distribution pattern and isotopic abundances were similar and coincident with the simulation results calculated by the software of API 'Isotopic Distribution Calculation' (Analyst, version 1.4.1, MDS Sciex, Ontario, Canada). This finding is in agreement with our earlier report which showed that highest intensity peak was mainly contributed from the stable isotope Sn-120 (Yang et al., 2010). However, in this case, isotopic composition of sulfur and tin were significantly complicated the MS spectra of $Sn(ECD)_2$-Et and $Sn(ECD)_2$ for determining of a fragmentation ion's molecular weight and m/z.

No significant DPs of $Sn(ECD)_2$-2Et was found in the MS spectra.

3.5.3 Degradation products, DP#6' and DP#7'

In the ECD to SnCl2 ratio of 2 : 1 (v/v), only two high polarity products at t_R of 0.93 and 1.14 min were left (Fig. 4(e)). It indicated that they might be partial degradation products of DP#4 and DP#5 when compared to the spectra of lower $SnCl_2$ solution (Fig. 4(d)). The typical product ion spectra and fragments of protonated molecular ions are shown in Fig. 5(k)-5(l) and summarized in Table 2. Three possible structures of Sn(ECD) (DP#6, DP#6' and DP#6'') and Sn(ECD)-Et (DP#7, DP#7' and DP#7'') are proposed in Fig. 1, of which

$Sn^{4+}(ECD)_{S2N2}$ (DP#6′) and $Sn^{4+}(ECD)_{S2N2}$-Et (DP#7′) were considered to be the prominent ones.

The experimental values of protonated molecular ions at m/z_{exp} = 442.11 and 414.30 supported this consideration. Moreover, there might be two possible explanations for this result.

First, the proposed net reactions of Sn(II) to Sn(IV) in the existence of dissolved oxygen or H_2O_2 are spontaneous in the forward direction. The proposed net reactions are as follows:

$$\frac{1}{2}O_2 + 2H^+ + Sn^{2+} \rightarrow H_2O + Sn^{4+} \quad E_{net} = 1.090 \text{ volt}$$

or

$$H_2O_2 + 2H^+ + Sn^{2+} \rightarrow 2H_2O + Sn^{4+} \quad E_{net} = 1.625 \text{ volt}$$

Second, both sulfur and nitrogen have lone pair electron can donate to the electrophile, Sn(IV). Sulfur is more nucleophilic than nitrogen, therefore sulfur can bond to the electrophile and react with it faster than the nitrogen does. For an irreversible reaction, the molecules do not have a chance to find the most energetically stable formation, and so they stay in whatever shape they form first and nucleophiles determine what the products are (A Crystal Clear Chemistry Concepts Tutorial). Highest amounts of DP#6′was existed in the ratio of ECD to $SnCl_2$ = 2 : 1 (v/v) and duration time of 4-7 hrs. Additionally, DP#7′ was existed only when the ratio of ECD to $SnCl_2$ (w/w) was greater than 2:1 and duration time was longer than 2 hrs. These results indicated that DP#6′ and DP#7′ were reversible thermodynamic products. Proposed CAD fragmentation pathways of the protonated molecules of DP#6′ and DP#7′ are shown in Fig. 6(b) and 6(f), respectively.

No significant DPs of $Sn(ECD)_{S2N2}$-2Et was found.

3.5.4 Degradation product, DP#8

Surprisingly, m/z 872.1, 901.0 and 975.5 can be found in the precursor scan of m/z 441.0, indicating that ECD trimer might be existed. Although no significant $Sn(ECD)(ECD)_2$ (mw_{avg} = 1086.05) can be detected in the MS spectra, it is reasonable to suggest a feasible structure and formation of DP#8 (trimer), i. e. $Sn(ECD)(ECD)_2$ shown as in Fig. 7. It seems that these results are due to labile and further decomposition of $Sn(ECD)(ECD)_2$.

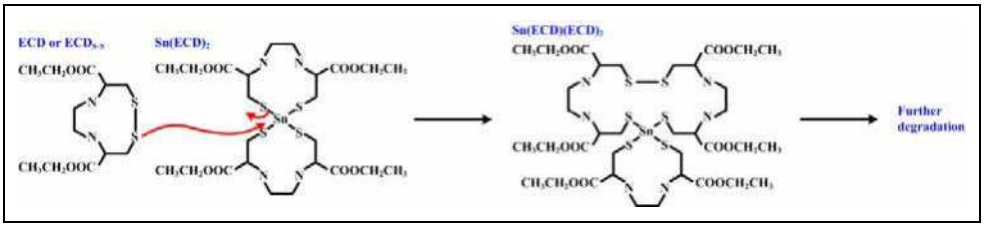

Fig. 7. Proposed formation mechanism of DP#8, $Sn(ECD)(ECD)_2$

3.6 Postulated degradation pathway of ECD and ECD Kit

The degradation pathway of ECD (API) and ECD Kit is shown in Fig. 8. Under alkaline and oxidation conditions, the drug can form DP#1, DP#1′, DP#2 and DP#2′ through ester hydrolysis and intra-molecular disulfidation. Under oxidation conditions, inter-molecular

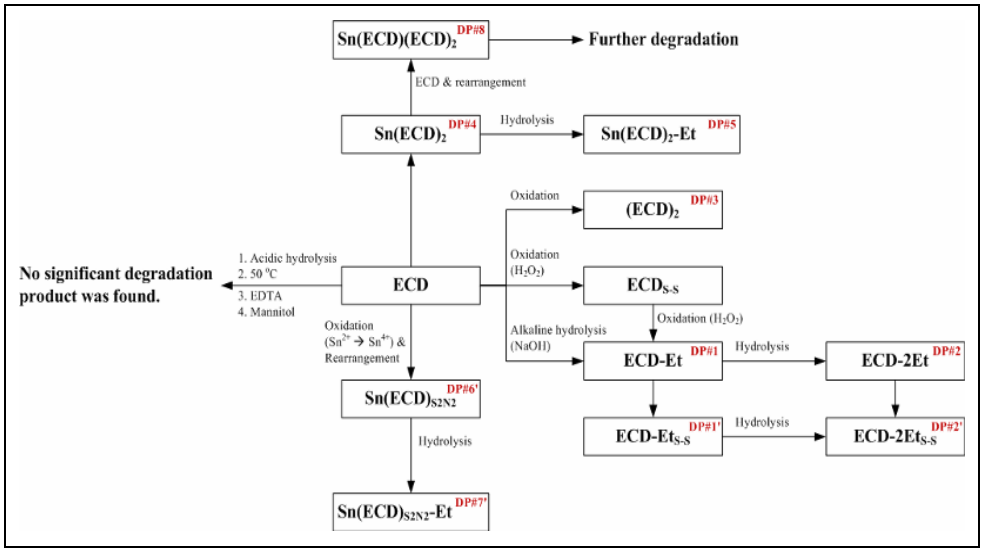

Fig. 8. Degradation pathway of ECD (API) and ECD Kit (drug product)

disulfidation of ECD also resulted in the formation of DP#3, i.e. $(ECD)_2$. For ECD Kit, the existence of $SnCl_2$ inhibited the formation of DP#1, DP#1′, DP#2 and DP#2′. In the meantime, oxidation of Sn(II) to Sn(IV) promoted the Sn(IV)-ECD complexation with coordination number of 1 and 2 to DP#6′ and DP#4, respectively. DP#6′ and DP#4 was further hydrolyzed to monoacid monoester derivatives, i.e. DP#7′ and DP#5. Moreover, the detection of Sn-trimer demonstrated the existence of DP#8, i.e. $Sn(ECD)(ECD)_2$.

4. Conclusion

The present study was designed to determine the factors affecting on the stability of ECD and ECD Kit and was given an account and the reasons for the use of Tc-99m-ECD which are suggested in practice guideline of ACR and EANM. The most interesting results emerging from the data are the degradation mechanisms and profiles of ECD. These findings enhance our understanding of ECD Kit about its stability, degradation pathways and structures of DPs. ECD is one of the diaminodithiol (DADT) derivatives to form stable complexes with radiorhenium or radiotechnetium. Therefore, the present study makes important implications for developing formulation of radiorhenium or radiotechnetium labeling pharmaceuticals. Further study for designing a more stable ECD Kit, such as a new reducing agent, reduction methodology or procedure is strongly recommended.

5. References

Abdel-Dayem, H. M. (Principal Drafter). (2002). ACR Practice Guideline for the Performance of Single-Photon Emission Computed Tomography (SPECT) Brain Perfusion Imaging, The American College of Radiology, (2002), Res. 19, pp. 487-491

Alsante, K. M., Ando, A., Brown, R., Ensing, J., Hatajik, T. D., Kong, W. & Tsuda, Y. (2007). The Role of Degradant Profiling in Active Pharmaceutical Ingredients and Drug Products. *Advanced Drug Delivery Reviews,* Vol.59, (2007), pp. 29-37, ISSN 0169-409X

Baertschi, S. W. (2006). Analytical Methodologies for Discovering and Profiling Degradation-Related Impurities. *Trends in Analytical Chemistry,* Vol.25, No.8, (2006), pp. 758-767, ISSN 0165-9936

Bauer, M., Silverman, D. H. S., Schlagenhauf, F., London, E. D., Geist, C. L., van Herle, K., Rasgon, N., Martinez, D., Miller, K., van Herle, A., Berman, S. M., Phelps, M. E. & Whybrow, P. C. (2009). Brain Glucose Metabolism in Hypothyroidism: A Positron Emission Tomography Study before and after Thyroid Hormone Replacement Therapy. *Journal of Clinical Endocrinology & Metabolism,* Vol.94, No.8, (2009), pp.2922-2929, ISSN 0021-972X

Borroni, B., Anchisi, D., Paghera, B., Vicini, B., Kerrouche, N., Garibotto, V., Terzi, A., Vignolo, L. A., Di Luca, M., Giubbini, R., Padovani, A. & Perani, D. (2006). Combined 99mTc-ECD SPECT and Neuropsychological Studies in MCI for the Assessment of Conversion to AD. *Neurobiology of Aging,* Vol.27, (2006), pp. 24-31, ISSN 0197-4580

Caroli, A., Geroldi, C., Nobili, F., Barnden, L. R., Guerra, U. P., Bonetti, M. & Frisoni, G. B. (2010). Functional Compensation in Incipient Alzheimer's Disease. *Neurobiology of Aging,* Vol.31, (2010), pp. 387-397, ISSN 0197-4580

Chang, C. -P., Shiau, Y. -C., Wang, J. -J., Ho, S. -T. & Kao, A. (2002). Abnormal Regional Cerebral Blood Flow on 99mTc ECD Brain SPECT in Patients with Primary Sjögren's Syndrome and Normal Findings on Brain Magnetic Resonance Imaging. *Annals of the Rheumatic Diseases,* Vol.61, (2002), pp. 774-778, Online ISSN 1468-2060

Chao, M. -Y., Liu, K. -T., Hsia, Y. -C., Liao, M. -H. & Shen, L. -H. (2011). Direct Determination of ECD in ECD Kit: a Solid Sample Quantitation Method for Active Pharmaceutical Ingredient in Drug Product. *Journal of Biomedicine and Biotechnology, in press*, ISSN 1110-7243

Chen, W. -Y., Lin, C. -Y., Chou, I -C., Tsai, F. -J. & Sun, S. -S. (2003). The Role of 99mTc-ECD Brain SPECT in Differentiating Tourrette's Syndrome from Chronic Tic Disorder. *Annals of Nuclear Medicine and Sciences,* Vol.16, (2003), pp. 59-63, ISSN 1022-923X

Diler, R. S., Reyhanli, M., Toros, F., Kibar, M. & Avci, A. (2002). Tc-99m-ECD SPECT Brain Imaging in Children with Tourett's Syndrome. *Yonsei Medical Journal*, Vol.43, No.4, (2002), pp. 403-410, ISSN 0513-5796

Jocić, B., Zečević, M., Živanović, L., Protić, A., Jadranin, M. & Vajs, V. (2009). Study of Forced Degradation Behavior of Eletriptanhydrobromide by LC and LC–MS and Development of Stability-Indicating Method. *Journal of Pharmaceutical and Biomedical Analysis,* Vol.50, (2009), pp. 622-629, ISSN 0731-7085

Kapucu, Ö. L., Nobili, F., Varrone, A., Booij, J., Vander Borght T., Någren, K., Darcourt, J., Tatsch, K. & Van Laere, K. J. (2009). EANM Procedure Guideline for Brain Perfusion SPECT Using 99mTc-Labelled Radiopharmaceuticals, Version 2, *European Journal of Nuclear Medicine and Molecular Imaging,* Springer, Published online: 17 October 2009.

Kulikov, A. U. & Zinchenko, A. A. (2007). Development and Validation of Reversed Phase High Performance Liquid Chromatography Method for Determination of

Dexpanthenol in Pharmaceutical Formulations. *Journal of Pharmaceutical and Biomedical Analysis*, Vol.43, (2007), pp. 983-988, ISSN 0731-7085

Liu, K. -T., Yang, H. -H., Hsia, Y. -C.; Yang, A. -S., Su, C. -Y., Lin, T. -S. & Shen, L. -H. (2008). Development and Validation of an HPLC Method for the Purity Assay of BZM, the Precursor of Striatal Dopaminergic D2/D3 Receptor SPECT Imaging Agent [123I]IBZM (Iodobenzamide). Journal of Food and Drug Analysis, Vol.16, No.5, (2008), pp. 28-38, ISSN 1021-9498

Mikiciuk-Olasik, E. & Bilichowski I. (2000). Determination of L,L-ethylene Dicysteine Di-Ethylester Stability by RP HPLC. *Chemia Analityczna (Warsaw),* Vol.45, (2000), pp. 809-813, ISSN 0009-2223

Raijada, D. K., Prasad, B., Paudel, A., Shah, R. P. & Singh, S. (2010). Characterization of Degradation Products of Amorphous and Polymorphic Forms of Clopidogrelbisulphate under Solid State Stress Conditions. *Journal of Pharmaceutical and Biomedical Analysis,* Vol.52, (2010), pp. 332-344, ISSN 0731-7085

Schraml, F. V., Beason-Held, L. L., Fletcher, D. W. & Brown, B. P. (2006). Cerebral Accumulation of Tc-99m Ethyl Cysteinate Dimer (ECD) in Severe, Transient Hypothyroidism. *Journal of Cerebral Blood Flow & Metabolism,* Vol.26, (2006), pp. 321-329, ISSN 0271-678X

Shah, R. P. & Singh, S. (2010). Identification and Characterization of a Photolytic Degradation Product of Telmisartan Using LC–MS/TOF, LC–MSn, LC–NMR and on-Line H/D Exchange Mass Studies. *Journal of Pharmaceutical and Biomedical Analysis*, Vol.53, (2010), pp. 755-761, ISSN 0731-7085

Shah, R. P., Sahu, A. & Singh, S. (2010). Identification and Characterization of Degradation Products of Irbesartan Using LC-MS/TOF, MSn, on-Line H/D Exchange and LC-NMR. *Journal of Pharmaceutical and Biomedical Analysis*, Vol.51, (2010), pp. 1037-1046, ISSN 0731-7085

Sun, S. -S., Chou, I -C., Lai, Y. -H. & Kao, C. -H. (2001). 99mTc-ECD SPECT Image in Children with Gilles de la Tourette's Syndrome: a Preliminary Report. *Annals of Nuclear Medicine and Sciences,* Vol.14, (2001), pp. 149-153, ISSN 1022-923X

Sunada, I., Ishida, T., Sakamoto, S. & Tsuyuguchi, N. (2004). A Discrepancy between Tc-99m HMPAO SPECT and Tc-99m ECD SPECT in Creutzfeldt-Jacob Disease. *Journal of Clinical Neuroscience,* Vol.11, No.6, (2004), pp. 648-650, ISSN 0967-5868

The Difference between Nucleophiles and Bases, *A Crystal Clear Chemistry Concepts Tutorial*, Date of access: 2011/4/7, Available from: http://www.crystalclearchemistry.com /organic/concepts/nucbase.php

Tsopelas, C. & Smyth, D. (2005). Characterization and Quality Control Analysis of 99mTc-Bicisate. *Journal of Nuclear Medicine Technology,* Vol.33, No.2, (2005), pp. 89-93, ISSN 0091-4916

Ukisu, R., Kushihashi, T., Tanaka, E., Baba, M., Usui, N., Fujisawa, H. & Takenaka, H. (2006). Diffusion-Weighted MR Imaging of Early-Stage Creutzfeldt-Jakob Disease: Typical and Atypical Manifestations. *RadioGraphics,* Vol.26, (2006), pp. S191-S204, Published online: www.rsna.org/education/rg_cme.html., Online ISSN 1527-1323

Verduyckt, T., Kieffer, D., Huyghe, D., Cleynhens, B., Verbeke, K., Verbruggen, A. & Bormans, G. (2003). Identity Confirmation of 99mTc-MAG3, 99mTc-Sestamibi and

99mTc-ECD Using Radio-LC-MS. *Journal of Pharmaceutical and Biomedical Analysis,* Vol.32, (2003), pp. 669-678, ISSN 0731-7085

Wielepp, J. P., Burgunder, J. -M., Pohle, T., Ritter, E. P., Kinser, J. A. & Krauss, J. K. (2001). Deactivation of Thalamocortical Activity is Responsible for Suppression of Parkinsonian Tremor by Thalamic Stimulation: A 99mTc-ECD SPECT Study. *Clinical Neurology and Neurosurgery,* Vol.103, (2001), pp. 228-231, ISSN 0303-8467

Yang, H. -H., Liu K. -T., Hsia Y. -C., Chen, W. -H., Chen, C. -C., Men, L. -C. & Shen, L. -H. (2010). Development and Validation of an HPLC Method for Determination of Purity of Sn-ADAM, a Novel Precursor of Serotonin Transporter SPECT Imaging Agent I-123-ADAM. *Journal of Food and Drug Analysis,* Vol.18, No.5, (2010), pp. 307-318, ISSN 1021-9498

Wide Spectra of Quality Control

Edited by Dr. Isin Akyar

ISBN 978-953-307-683-6
Hard cover, 532 pages
Publisher InTech
Published online 07, July, 2011
Published in print edition July, 2011

Quality control is a standard which certainly has become a style of living. With the improvement of technology every day, we meet new and complicated devices and methods in different fields. Quality control explains the directed use of testing to measure the achievement of a specific standard. It is the process, procedures and authority used to accept or reject all components, drug product containers, closures, in-process materials, packaging material, labeling and drug products, and the authority to review production records to assure that no errors have occurred.The quality which is supposed to be achieved is not a concept which can be controlled by easy, numerical or other means, but it is the control over the intrinsic quality of a test facility and its studies. The aim of this book is to share useful and practical knowledge about quality control in several fields with the people who want to improve their knowledge.

How to reference

In order to correctly reference this scholarly work, feel free to copy and paste the following:

Kung-Tien Liu, Yu-Yung Lin, Yi-Chih Hsia, Jian-Hua Zhao, Chang-Yung Su, Shang-Yu Shen, Lee-Chung Men and Lie-Hang Shen (2011). Study of Degradation Products and Degradation Pathways of ECD and Its Drug Product, ECD Kit, Wide Spectra of Quality Control, Dr. Isin Akyar (Ed.), ISBN: 978-953-307-683-6, InTech, Available from: http://www.intechopen.com/books/wide-spectra-of-quality-control/study-of-degradation-products-and-degradation-pathways-of-ecd-and-its-drug-product-ecd-kit

INTECH
open science | open minds

InTech Europe
University Campus STeP Ri
Slavka Krautzeka 83/A
51000 Rijeka, Croatia
Phone: +385 (51) 770 447
Fax: +385 (51) 686 166
www.intechopen.com

InTech China
Unit 405, Office Block, Hotel Equatorial Shanghai
No.65, Yan An Road (West), Shanghai, 200040, China
中国上海市延安西路65号上海国际贵都大饭店办公楼405单元
Phone: +86-21-62489820
Fax: +86-21-62489821